International Journal of Computational and Experimental Science and ENgineering
(IJCESEN)

Vol. 11-No.3 (2025) pp. 5204-5223
http://www.ijcesen.com

ISSN: 2149-9144

Research Article

An Advanced Feature Fusion and Subject- Feature Fusion with Contrast Enhancement Model for Osteoporosis Detection in Femur Bone

Dhanyavathi A.[1,2*], Veena M. B.[3]

[1]Research Scholar, Visvesvaraya Technological University, Belagavi-590018, Karnataka, India.
[2]Assistant Professor, EEE Department, Dr. Ambedkar Institute of Technology, Bengaluru-560056, Karnataka, India.
***Corresponding Author Email:** dhanyavathia@gmail.com - **ORCID:** 0009-0001-6750-5172

[3]Professor, Department of Electronics and Communications, BMS College of Engineering, Bengaluru, Affiliated to Visvesvaraya Technological University , Belagavi-590018, Karnataka, India.
Email: veenamb.ece@bmsce.ac.in - **ORCID:** 0000-0001-9171-2625

Article Info:

DOI: 10.22399/ijcesen.3318
Received : 12 May 2025
Accepted : 10 July 2025

Keywords

Osteoporosis;
Dual Energy X-ray Absorptiometry;
Bone Mineral Density;
X ray images;
augmentation;
fusion strategy.

Abstract:

Osteoporosis causes the mineral density of bones to decrease, the bones become more porous and fragile, which increases the risk of fracture. Dual Energy X-ray Absorptiometry (DEXA) detects bone mineral density (BMD) effectively, it is the most widely used method for diagnosing osteoporosis. Despite DEXA's efficacy in determining BMD, some disadvantages of the technology included size, expense, and limited availability. To overcome these issues, the medical image based osteoporosis diagnosis was done. Yet those models also have some impacts like poor feature extraction and low contrast. The best way to diagnose osteoporosis was analyzed both BMD and images at a time. This merging model provided a better outcome but the linkage of both images and subject values was most complicated and take too much of time. In proposed work, a fusion strategy based detection approach was designed to predict osteoporosis in femur bone. The proposed model have three stages namely feature extraction, feature fusion and subject-feature fusion. The collected X ray images and its subject record were collected and split separately for accurate prediction. Pre-processing and augmentation process were done to improve the image information. Then, extract the images using two different methods and fused both features. Further, the subject records were fused with its appropriate features to detect the osteoporosis disease appropriately using a deep learning approach. The proposed model provides 97% accuracy with 7% false positive rate and compared to another traditional models. The suggested approach detects osteoporosis effectively so it was well suitable for real-time applications.

1. Introduction

Osteoporotic fractures (OF), a severe side effect of osteoporosis, are fractures that occurs during daily tasks or minor trauma [1]. Numerous fractures caused by osteoporosis include those of the femur, vertebrae, distal radius, hip, and proximal humerus [2]. Osteoporosis is estimated to cause an OF every three seconds, resulting in over nine million new fractures annually; one-fifth of men and one-third of women will experience osteoporosis at sometime in their lives [3]. Osteoporosis can be excruciating, deadly, highly incapacitating, and a drain on families and society. Patients' quality of life is gravely compromised [4]. The chance of fracture is decreased in osteoporosis patients who use therapy strategies such as medication, lifestyle changes, and fall prevention [5]. Osteoporosis must be prevented by accurately identifying those at risk early on and implementing effective preventive measures in a timely basis [6].A bone mineral density (BMD) test is most frequently used to diagnose osteoporosis. It is frequently used to diagnose low BMD or osteoporosis [7]. Additionally, therapeutic practice frequently fails to recognize osteoporosis [8]. However, the BMD test by itself cannot accurately predict osteoporosis. Additionally, the BMD test limited clinical application is constrained by its high expense, exposure to radiation exposure, and poor mobility [9]. The primary method of diagnosing osteoporosis at this time is dual-energy X-ray absorptiometry, or DXA [10]. With only around 0.95

percent of people over 50 using it each year, the DXA value for diagnosing osteoporosis is incredibly low [11]. Hence, it is encouraged to develop prediction models that incorporate a number of risk factors to detect osteoporosis in several clinical guidelines. Yet, there are a lot of additional things that can affect the diagnosis, like age and a history of fragility fractures.

As computer technology and artificial intelligence (AI) techniques have advanced recently, computer-aided diagnostic (CAD) systems that may aid in the differential diagnosis of osteoporosis by employing medical images are appearing more frequently in the literature [12]. The commonly employed methods, which include quantitative computed tomography (QCT), dual-energy X-ray absorptiometry (DXA), and quantitative ultrasound (QUS), as well as trying to cut imaging methods, like dual-layer spectral CT, HMRS, and positron emission tomography (PET), are used to evaluate osteoporosis [13]. BMD as determined by DXA using two-dimensional structures is equal to the sum of cortical and cancellous bone. However, DXA was unable to totally exclude the impact of cortex, hyperosteogeny, and sclerosis on BMD assessment, which may underestimate the true loss of bone mass [14]. In recent years, texture features have been used often in image classification, and a few research have been performed to identify the appropriate texture features in osteoporosis diagnosis utilizing bone radiograph images [15]. Problems arise, however, because an osteoporosis patient's images are extremely similar to those of healthy individuals. The usual texture features cannot be utilized to classify them in a way that is suitable to humans and they are not visible to the naked eye. For image-based diagnosis, a low-cost system with high performance is therefore highly desired [16].

BMD measurements and X ray images are two of the finest ways to diagnose osteoporosis in a patient [17]. Due to the fact that both X ray images and BMD values are used to detect osteoporosis individually. Nevertheless, combining BMD values and X ray images takes time and is challenging since the data must be combined to create an appropriate X ray image or the diagnosis would be incorrect. In attempt to mitigate these effects, some strategies that include both subject matter and images have recently been developed. Traditional methods include drawbacks such as ineffective contrast, slow prediction, inappropriate fusion, and inadequate image information. To overcome these limitations, a novel feature fusion and merging subject record with suitable images was introduced. The proposed model have three phases, first the features were extracted from X ray images using convolution features extractor and GLSDM, second both features are fused to convert single features, and the third one is fusing features with its corresponding subject record. The osteoporosis disease identification in femur bone was crucial in the medical world, the objectives of the proposed model was discussed as follows.

- An advanced features fusion and subject-feature fusion strategy based prediction model is designed to detect osteoporosis in femur bone.
- Medical data are collected from clinic that contain radiography images with its subject details. Then, the X ray images and subject details are separated for further procedure.
- The raw radiography images are undergone a pre-processing step to increase the information and contrast quality of the images.
- After pre-processing, the data are augmented to rotate 30o, 45o, 60o and 90o which was most useful for improving prediction accuracy.
- The important features from the augmented images are extracted under two processes such as convolution feature extraction and Gray level spatial dependence matrix.
- Then, fuse the two features to converter a single feature for a X ray image, further the subject record was fused with its corresponding features to make an effective prediction performance.
- DNN classifier is utilized to predict an appropriate condition of osteoporosis in the fused data. Additionally, the performance was established by comparison with a few other current methods.

The manuscript is organized as follows for the remaining portions: section 2 lists the relevant research for the suggested model. The overall strategy and methodology for the suggested work are described in Section 3. Section 4 presents the performance validation of the proposed framework. At last, the overall conclusion of the work is provided in section 5.

2. Related work for detecting osteoporosis

Characteristics of the relatively common condition osteoporosis include low bone mineral density and an increased risk of fracture, known as an osteoporotic fracture. Bone fracture risk is considerably reduced by osteoporosis early diagnosis. Notably, bone mineral density values and medical images were utilized to diagnose this disease. Some of the recently developed osteoporosis prediction models are discussed as follows. Prakash et al. [18] had invented a method for detecting osteoporosis as early as feasible by combining models and algorithms. For osteoporosis diagnosis and prediction, a number of models and algorithms was used rather than relying solely on one to provide the best results. Thus, a system that employs multiple algorithms for disease prediction. Although this system is efficient, it is difficult to learn and has high maintenance costs. Jang et al. [19] had created a deep neural network model to predict osteoporosis from basic hip radiography, and by leveraging the most recent advancements in the area of medical artificial intelligence, it might be utilized as a screening tool for the condition. Though these forecasts occasionally might not be accurate osteoporosis predictions, the neural network model performed well in predicting osteoporosis.

Sato et al. [20] created a deep learning trained model using a large dataset collected from numerous institutions to predict BMD and diagnosis based on the T-score using age, sex, and chest X-rays. In the event that models with high predicted accuracy are created, chest X-rays can be employed as a bone screening method. Although there is need for improvement, this technique is effective in terms of prediction. Sollmann et al. [21] presented recommendations on quantitative MRI methods and associated outcomes in terms of osteoporosis at the proximal femur and spine from a clinical and scientific standpoint. The efficacy of this system is partly attributed to scant evidence of distinctly enhanced fracture prediction.Yamamoto et al. [22] stated that osteoporosis diagnosis can be improved with a statistically significant difference by merging image features with patient factors. Although a significant difference like this would highlight the value of taking patient factors into consideration and advance the field of AI diagnostic research in osteoporosis, the system's lengthy decision-making process renders it ineffective. Du et al. [23] established a model for the supplementary diagnosis of conditions linked to osteoporotic fractures of the femur neck in the elderly. Based on the X-ray image processing technique to enhance the effectiveness and performance of such illness screening in certain populations. However, this system not predict accurately due to the reduction of additional information from the image data.

Dadsetan et al. [24] developed a machine learning-based computer model to perform radiomics on clinically accessible X-ray images to determine the risk of osteopenia and osteoporosis. This study's shortcomings include its inadequate output metrics value and AUC. Shahzad et al. [25] suggested preprocessing X-ray images to find errors using the RADTorch package and using a learning model based on a ResNet50 and XGBoost Classifier to predict osteoporosis in the MURA V2 dataset. Despite its efficiency, this system's inadequate image quality severely limits its possibilities.

Slaidina et al. [26] offered a model for examining the potential impact of overall BMD changes on the menopausal women's second and third cervical vertebrae GVs, which are assessed using cone beam computed tomography images; the study additionally examined the CT images to determine the risk of osteoporosis in these women. However, cone beam CT imaging is typically not advised for predicting osteoporosis. Hsu et al. [27] had suggested a Two-Compartment Model to quantitatively assess the lumbar spine vBMD and bone volume fraction (BVF). The relationships between gender, age, and BMD were examined in addition to the wide use of TCM in the diagnosis of osteoporosis and osteopenia. The results, however, may not be sufficient to accurately identify the illness. The above mentioned related work focus on osteoporosis. However, these models have several shortcomings, such as high cost and inaccurate prediction [23], [24], [26], [27], [28], potential is poor [21], [22], [23] and reduction of additional information from the image data. In order to overcome these issues, a novel feature fusion and merging subject record with suitable images should be introduced in the proposed model. A clear discussion of the proposed model architecture and its working principles are presented as follows.

3. Proposed feature and image fusion model for predicting osteoporosis in femur bone

Osteoporosis is known as a "silent" illness as it typically doesn't cause any symptoms until a bone breaks. When there are abnormalities in the structure of bone tissue and excessive bone mass loss, osteoporosis develops. For many years, the clinical reference standard for determining fracture risk and diagnosing osteoporosis has been dual-energy X-ray absorptiometry or DEXA. However, the issue with DEXA records is that they does not provide a realistic prediction of bone strength and fracture risk always. So, medical images were utilized to detect osteoporosis, yet those also have some impacts for detecting the disease. The best estimation of bone strength would probably be obtained if bone structure and bone mineral density could be measured simultaneously. In the proposed work, a novel feature fusion and image-text fusion with contrast enhancement technique is developed to detect osteoporosis. The proposed model provides an effective prediction performance because it have both BMD and image combination for a patient. Also, various pre-processing approaches are utilized for contrast enhancement of radiography images. Figure 1 illustrates the general schematic model of the proposed approach.

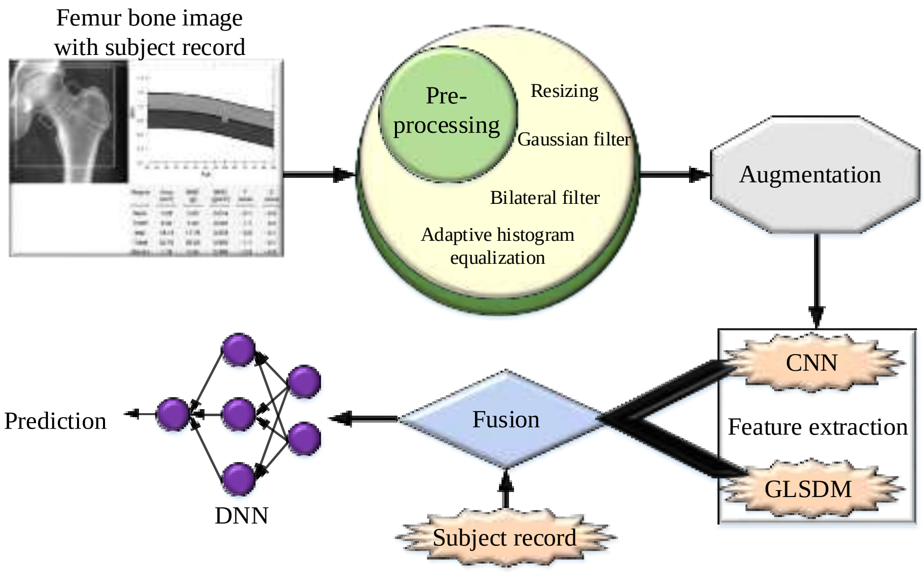

Figure 1. *Architecture of proposed feature fusion and image-subject fusion methodology.*

The working process of the proposed methodology for detecting osteoporosis in femur bone is illustrated in Figure 1. It demonstrates the raw data of femur bone radiography images with their subject matter of patients are collected from a clinic. For accurate analysis, separate the subject record and radiography image data. The image data are pre-processed because they contain noise and irrelevant elements that may affect the prediction process as well as consume more time. The pre-processing techniques are resizing, Gaussian filter, bilateral filter, adaptive histogram equalization that are employed in the proposed model. Pre-processing techniques have the advantage of increasing image quality and accuracy. After that, the augmentation process is done from the pre-data. The augmentation process rotates the images to a predetermined degree using the pre-data that was applied. Afterwards, the augmented femur bone data's features are extracted. Here, two methods are individually used to extract the features for better prediction performance. Two techniques for extraction include a grey-level spatial dependency matrix (GLSDM) and a convolutional neural network (CNN). With GLSDM, it was discovered that colour features are more effective in identifying true positives. CNN's main advantage is its ability to generate the required features from time series data and frequency representation images. False positives are less common when GLSDM characteristics are used, though. The subject record and the features obtained are then integrated, and the classification process is then carried out. Using a deep neural network (DNN) classifier, the exact state of the input data will be known during the classification process.

1.1. Pre-processing

Image pre-processing procedures are necessary to improve the raw input image's quality and eliminate noise. The pre-processing stage is the most significant to remove the problems of the image without affecting the information of an image. In the suggested model, the comparison of radiography images of the femur bone is improved by applying four distinct pre-processing procedures. The methods used for quality improvement is resizing, Gaussian filter, bilateral filter and adaptive histogram equalization. The below section clearly explains the pre-processing technique.

i. Resizing

Image resizing is a method for altering the size of the images with a specified range (256*256). It assists in decreasing the pixel size of an image, resulting in a number of advantages, such as lowering the neural network's training period. Each image is scaled and resized into a constant size. The resizing is described by the formula below.

$$I(x,y) = \sum_{i=0}^{3}\sum_{j=0}^{3} a_{ij} m^i n^j \quad (1)$$

Where m denotes pixel width, n signifies pixel height, and a_{ij} square area of the femur bone images.

ii. Gaussian filter

An image's detail and noise level can be improved with the Gaussian low-pass filter, which is widely used in image processing applications. A smoothing technique called the Gaussian filter is used to reduce noise and enhance the sharpness of the femur bone image. Due to its capacity to develop a probability distribution for data or noise and its function as a smoothing operator, the Gaussian function discovers widespread application. Equation 2 provides the Gaussian filter's broad mathematical expression.

$$G(x,y) = \frac{1}{2\pi\sigma^2} e^{\frac{x^2+y^2}{2\sigma^2}} \quad (2)$$

$G(x,y)$ represents the Gaussian filter value, σ is the standard deviation of the Gaussian distribution, and x and y stand for row and column. Significantly, the standard deviation affects the Gaussian filter's response [29].

iii. Bilateral filter

A bilateral filter is a type of non-linear, non-iterative filter used in image processing. The neighborhood pixel approach is used by the bilateral filter to calculate intensity distance and spatial distance. When Gaussian noise is present, the bilateral filter can be defined as follows. [30]

$$\widehat{f_1}\,(x) = \frac{\sum_{j\in\Omega} g_{\sigma_s}(j) g_{\sigma_r}\big(f(x-j)-f(x)\big) f(x-j)}{\sum_{j\in\Omega} g_{\sigma_s}(j) g_{\sigma_r}\big(f(x-j)-f(x)\big)} \quad (3)$$

In this case, the bilateral filter's output at position x is represented as $\widehat{f_1}\,(x)$. Bilateral filters are dependent on two regulating factors, σ_s and σ_r. The filtering process as a whole is affected by the two parameters, σ_s and σ_r. The bilateral filter increases noise variance and blurs the image due to Gaussian noise. Thus, selecting the regulating parameters σ_s and σ_r appropriately will enhance the quality of the bone image.

iv. Adaptive Histogram Equalization

One of the most widely used computer image pre-processing strategies for enhancing contrast in images is the Histogram Equalization (HE) algorithm. Less localized intensity difference (HE) results in increased contrast. It is possible to observe the intensity spreading values in an image as arbitrary values, ranging from 0 to $L-1$. The term cumulative distribution function (often related to itself) also refers to random computation. The probability that an arbitrary value will be assigned a value that is less than or equal to a specific value is determined by this function. Let f be the input image of the femur bone. The array of numerical pixels in the range of intensity values starts at 0 and ends at $L-1$. The adaptive HE model's numerical expression is as follows [31]:

$$pn = \frac{number\ of\ pixels\ with\ intensity\ n}{total\ number\ of\ pixels} \quad n = 0,1,\dots L-1 \quad (4)$$

In this case, p is the regularized histogram of the main image f and L denotes the intensity probability value. After completing the pre-processing stage, the images are further proceed for image augmentation. The benefit of using data augmentation is to improve deep learning robustness and overfitting.

1.2. Augmentation

Improving the quality of feature extraction from femur bone scans requires much data augmentation. In order to reduce the presence of class imbalance as well as to add more samples to the dataset, data augmentation is required. Data augmentation strengthens the model's ability to generalize by resulting in translation, perspective, size invariance, and artificial diversity of the analyzed dataset, in addition to increasing the sample count. The name of this transformation suggests that it involves rotating the original image to a specified angle. Supplementing a dataset with random rotations at various angles, such as multiples of 45° and from -15° to +15° or 10° to 175°, is a common occurrence. In the proposed study, obtaining adequate results requires obtaining medical images, which can be costly. Therefore, data augmentation is used to create many versions of femur bone images, thereby increasing the size of the dataset. The pre-data images of the femur bone are all rotated at exact angles of 30°, 45°, 60°, and 90° after the image quality has been improved. Although these enhanced femur bone images are similar to those in the original dataset, it contains more data that will let the classification system be wider used.

1.3. Feature extraction

Features are characteristics or patterns seen in an image that facilitate the identification of individual pixels. It explains how raw data is transformed into numerical features so that the original data set's contents may be processed. Compared to using artificial intelligence on the raw data directly, it results in better outcomes. In feature extraction separates and condenses a sizable collection of raw data into more manageable groupings. To increase the suggested model's prediction performance, two novel feature extraction techniques are used to extract the appropriate data from the femur bone. Initially, the augmented data are extracted using a deep learning model and in another side the features are extracted using a grey-level spatial dependence matrix (GLSDM). The combination of these features are more useful for detecting osteoporosis in the femur bone.

i. Convolution feature extraction

Densely Connected Convolutional Neural Network of 169 layers (DenseNet-169) has an initial convolution and pooling layer, three transition layers, and four dense blocks. Following these layers comes the last layer, referred to as the classification layer. Using stride 2, the first convolutional layer develops 7×7 convolutions, and then it utilizes stride 2 to execute a 3×3 max pooling. The network is then divided into three sets, one for each transition layer and dense block that follows. The DenseNets architecture is split into the several densely linked dense blocks that were previously described because the main goal of convolutional neural networks is to collect feature map sizes down. The feature maps from the previous levels has to be concatenated in order to proceed to the next layer, which is impossible unless every feature map has the same dimensions. The layers located between these dense blocks are known as transition layers. Each network transition layer is composed of up of a batch normalization layer, a 1×1 convolutional layer, and a 2×2 average pooling layer with a stride of 2. As previously stated, there are four dense blocks, with two convolution layers each. The first layer is sized 1 × 1, while the second is sized 3 × 3. DenseNet169 architecture pretrained on Image Net has four dense blocks with sizes of 6, 12, 32, and 32. The activation function obtains the value from the input layer by transferring features from the femur image into the convolution layer.

$$x^l = f\left(W^l x^l + b^l\right) \quad (5)$$

Where f is the activation function, W is the weight, l is the number of layers, and b is the offset. In the forward propagation stage, a learnable convolution kernel convolves multiple feature maps from the previous layer resulting in a new feature map with the activation function.

$$x_j^l = f\left(\sum_{i\epsilon M_j} X_i^{l-1} * k_{ij}^l + b_j^l\right) \quad (6)$$

The previous layer is represented by l, the first feature map of the current layer by $l-1$, and the j convolution kernel, which relates to the first feature map of the j previous layer, b_j^lan offset value is represented by x_j^l. These processes provide results that are not readily influenced by the feature or pixel's actual location within the image.

ii. Gray level spatial dependence matrix

The GLSDM is an efficient and cost-effective technique for describing texture information. It is based on statistical image analysis. Estimating texture features based on the relationship between two nearby pixels is the basic idea. A two-dimensional matrix of probabilities of interaction between pairs of pixels separated by a distance d in a specific directionθ is known as a GLSDM. By standardizing GLSDM by each set of pixels, the scale invariance of the texture pattern is calculated as follows [32]:

$$p_{d,\theta} = \frac{P_{d,\theta}\,(m,n)}{x_{all}} \quad (7)$$

$P_{d,\theta}\,(m,n)$ represents the joint probability of neighborhood groups of pixels in distance d and directionθ, where m,n are the luminances of those intensities. The total number of pixel pairings is calledx_{all}.The GLSDM Features used in this work are Correlation, Energy, Homogeneity, and Entropy. These features can be calculated as follows:

$$\text{Correlation} = \sum_{i,j=0}^{N-1} \frac{(i,j)P(i,j) - (\mu_x - \mu_y)}{\sigma_x \times \sigma_y} \quad (8)$$

$$\text{Energy} = \sum_{i,j=0}^{N-1} \sqrt{P(i,j^2)} \quad (9)$$

$$\text{Homogeneity} = \sum_{i,j=0}^{N-1} \frac{P(i,j)}{1+(i-j^2)} \quad (10)$$

$$\text{Entropy} = \sum_{i,j=0}^{N-1} P(i,j)\,(-\ln P(i,j)) \quad (11)$$

$P(i,j)$ is the element $(i,j)$of GLSDM, and N is the number of the component level in the image under quantization.

1.4. Fusion

Combining different data sets into a single source is the process known as data fusion. The suggested model used to combine features from femur bone radiography images with related subjects record. That is each femur image's features are extracted from two separate models that individual features are combined and the corresponding subject record of that images also combined to make a single data. The result of these combined process is high accuracy, more reliable operation and effective predictive performance. These fused data are further used for the prediction process.

1.5. Classification

The combined data are fed into a classifier as input to predict the disease, and this final step is referred to as the classification process. While there are several classifier models available, deep neural networks (DNNs) are preferred for prediction purposes in the proposed work. Models may learn complex features faster and perform more demanding computational tasks because of the several layers of deep neural networks.

i. DNN

As shown in Figure 2, an ANN that contains multiple hidden layers is expanded into a deep neural network (DNN). An arranged network of neurons in layers, a DNN performs basic calculations by utilizing input from layers above it . The layers are made up of nodes, which are effectively locations where computing happens. Every two-layer succession's unit pairs each have a unique bias and weight for every node [33]. DNN consists of three steps: input layer, hidden layer, and output layer. The DNN's input layer gathers the input data that is provided. The proposed model's input layer obtains input in the form of extracted features and recorded data. The input data is processed mathematically by the DNN hidden layer. In DNN, there are numerous hidden layers where the activation function works. The final layer, referred to as the output layer, has a significant connection with the target value that the model tries to forecast for the specific category of input data.

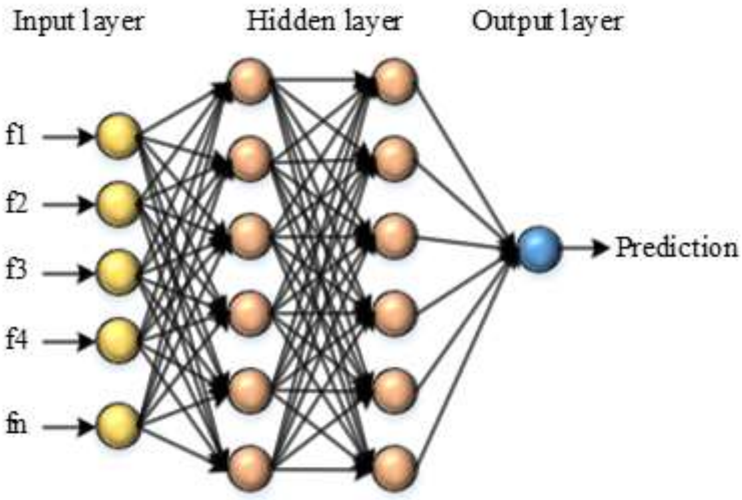

Figure 2. Proposed DNN model for osteoporosis prediction.

Let us assume that there are $n = 1, 2, .., n$ inputs, $f_1, f_2 .... f_n$; let us consider $H_1, H_2, ... H_k$ represents hidden layers, indicates the layer weight and takes into consideration the hidden neuron's bias, $B = 1, 2, .. n$. Where k varies from 1 to 2. The input layer's typical configuration is,

$$f_N = \left(\sum_{i=1}^{m} f_n \times w_{iN}^{I}\right) + B \tag{12}$$

The general phrase for a hidden layer is

$$H_k = \varphi^{(i)}\left(\sum_{j=1}^{N} w_{jN}^{h\,ij}\right) + B \tag{13}$$

The following expression is computed as the output:

$$y_i = \varphi^{(k)}(\textstyle\sum_j w_{ij}^{(i)} h_j^{(i)} + b_i^{(i)} \tag{14}$$

The input is represented by w, the output by y, the bias by b, the input units by f, the hidden layer units by H_k and the activation function by φ. Using this deep neural network classifier to predict the disease effectively from the femur bone image and its record. The Pseudocode of the proposed model is provided below,

Pseudocode for proposed osteoporosis detection

```
Osteoporosis dataset = B
Split dataset B: image = I and data = D
Begin
{
For all femur images in the dataset
    # Preprocessing
        R= Resizing (I)
        F= Gaussian filter (R)
        N= Bilateral filter (F)
        E= Adaptive histogram (N)
    # Augmentation
        S=Augmentation (E)
    # Feature Extraction
        A= CNN (S)
        C= GLSDM (S)
    # Fusion
        H= Fusion (A+C+D)
```

```
# Classification
    Data splitting
        {
            Training data
            Testing data
            Actual class
        }
    O= DNN (H)
}
End
Outcome: Predict whether the image is normal or osteoporosis
```

4. RESULT AND DISCUSSION OF PROPOSED MODEL OBSERVED VALUES

In this section an advanced feature fusion and text-image fusion with contrast enhancement model for osteoporosis detection in femur bone image is designed and its performance is analyzed. In the proposed work, a femur bone CT image is taken and it is pre-processed using re-sizing, Gaussian filter, and bilateral filter and adaptive histogram equalization. Pre-processing procedures to increase the effectiveness of the detection process by reducing unwanted elements in the images. Augmentation is utilized in the pre-data for rotating various angles to improve the prediction accuracy. Then, utilizing convolution features and GLSDM to extract useful features from the augmented data. To fuse useful extracted features and its subject record to make a prediction performance effectively. To attain an appropriate prediction of osteoporosis in the fused data, a DNN classifier is applied which analyzes the data and predicts the appropriate condition. The advanced model conclusion is implemented and performance is observed using MATLAB R2021b software on an Intel Core i7 CPU, NVIDIA GeForce RTX 3070 GPU, and 64GB RAM system.

i. Dataset description

A large image and annotation database is taken into consideration to aid in BMD measurement from DEXA images research. The database is created after the collection of 441 DEXA images from various patients. The database is created using the regions of the spine, left femur, and right femur that are extracted from the DEXA images. a preliminary effort to provide a collection of Dual Left Femur (LF) and Right Femur (RF) DEXA scan images, or DEXSIT. Through a meticulous examination of every single dexa scan image, DEXSIT provides an extensive annotation. Each bone image has the following properties manually annotated. Those of the data are Particular identification number (ID), gender, age, height (cm), weight (kg), dual femur (left and right): T-score, Z-score, BMD (g/cm2), area (cm2), fracture risk: fracture risk status for each femur bone.

Right and left femur bone images are taken for osteoporosis diagnosis. Separate the subject record from the image data for accurate analysis. Improving accuracy and information in the images using pre-processing procedure. Augmentation was done in the pre-data and further utilizing convolutional feature extraction and GLSDM to extract features. To fuse extracted features and its subject record by using a fusing mechanism. A DNN classifier is used to analyze the fused data and predict osteoporosis. In Table 1, the pre-processed output of the femur bone image is mentioned.

Table 1. *Output of pre-processed femur bone image*

Original image	Resizing	Gaussian filter	Bilateral filter	Adaptive HE
				
				

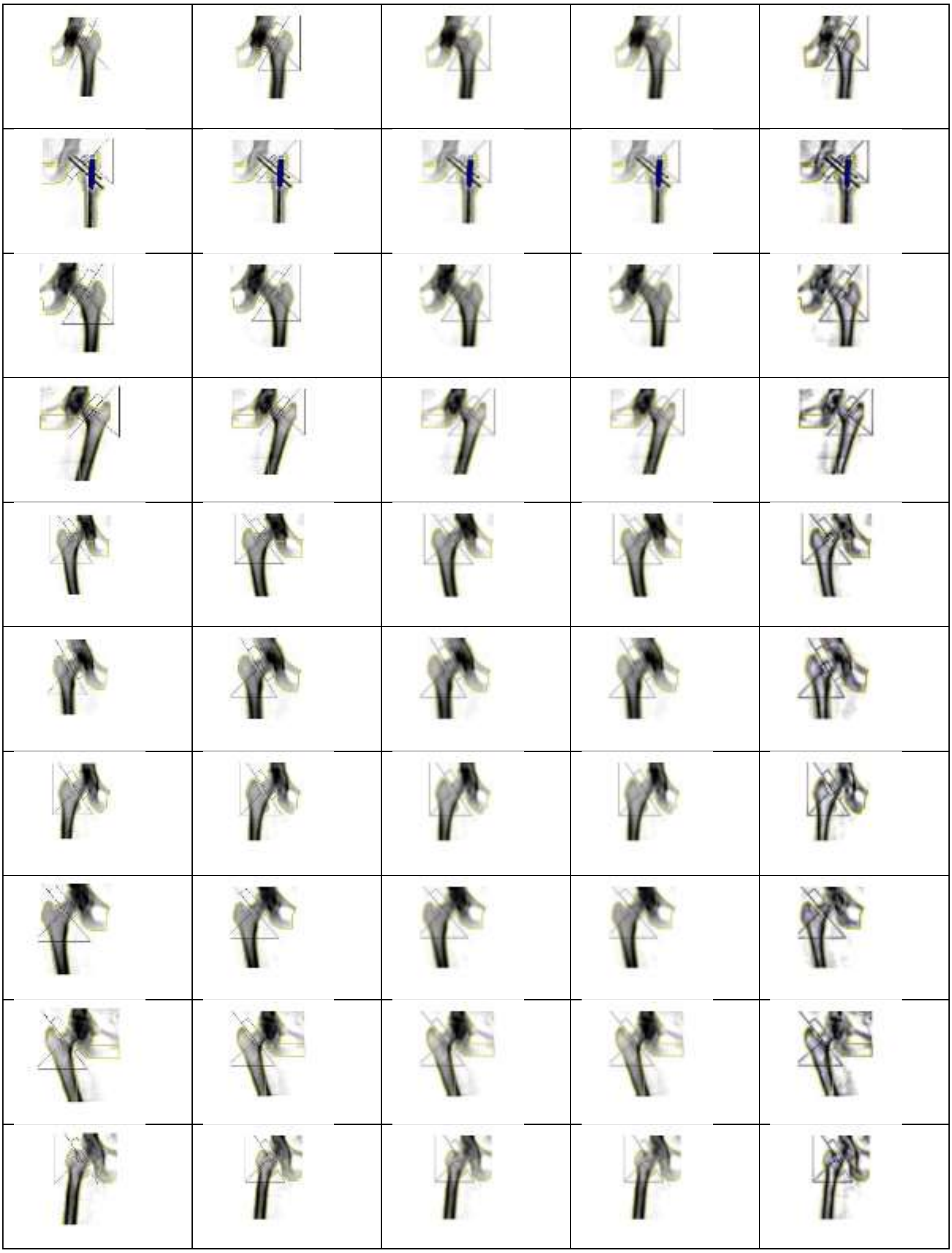

These pre-processed data which is given to the augmentation process. The augmentation process is used to improve the accuracy and prediction process. In augmentation, femur bone images are rotated in $30^0, 45^0$, 60^0 and 90^0 and observed that images. Feature extraction from augmented data using GLSDM and convolutional feature extraction. To combine the subject record and the extracted features using a fusing method. A DNN classifier is used to analyze the fused data and forecast whether the information provided is in its proper state. Proposed model fusion illustrations are shown below in Table 2.

Table 2. *Fusion images of femur bone extracted feature images*

Samples	Fused images
1	
2	
3	
4	
5	
6	

Feature fusion is widely used in many domains, such as image processing and classification. With feature fusion, the duplicate information is removed and the most discriminative information from numerous input features is extracted. In the proposed model, the fusion technique is used in femur bone images to make more information for appropriate osteoporosis detection. Both left and right images are fused to convert a single images and further the feature were extracted and merged with the subject record. The fused subject and feature data are given to the DNN classified to predict the appropriate condition of the images. Table 3 shows the simulation parameters of the proposed DNN and existing methods.

Table 3. *Simulation parameters of proposed and existing method*

Parameter	**Method**	**Range**
Max iteration	DNN	100
Step ratio		0.01
Batch size		0
Training accuracy	MLP	0
Size of the mini batch		128
Number of epochs		40
gamma	SVM	1
c		-1
G		tanh
Current node	RF	1
Free node		0,1

Min leaf	DT	5
Max split		381
Version		2
Method		tree
Type		regression

ii. Confusion matrix

A confusion matrix (CM) is typically used to illustrate how well a model performs on a particular batch of images in terms of categorization. It shows the classes that the model correctly and incorrectly predicts. The confusion matrix is a N x N matrix that is generated based on the classes, where N is the number of classes or outputs. The suggested model confusion matrix is shown in Figure 3. The true class value is 55 in the case of osteoporosis and 27 in the first class (normal). Proving that the recommended model has better prediction performance.

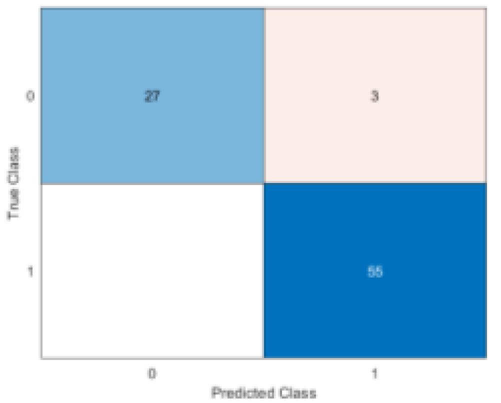

Figure 3. *Analysis of confusion matrix.*

iii. ROC curve

The receiver operating characteristic (ROC) curve demonstrates that an accurate diagnosis of osteoporosis can be obtained with X ray images and patient information. The ROC of the proposed model shows that well a classification model works throughout all classification thresholds that as shown in Figure 4. True Positive Rate and False Positives Rate were the two metrics used to plot this curve. The suggested model's ROC curve value is 1, indicating that it provides an efficient prediction procedure.

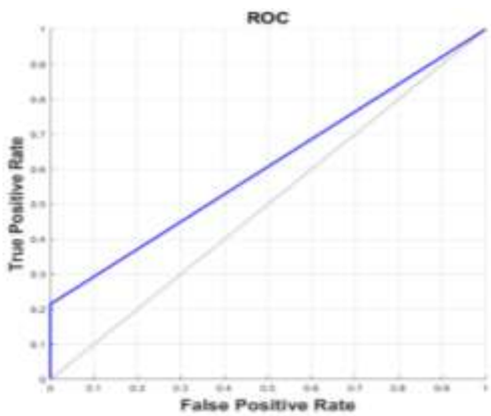

Figure 4. *Analysis of the ROC curve.*

1.6. Performance comparison

This section compares the proposed model's accuracy, sensitivity, specificity, precision, false positive rate, false negative rate, NPV, F1_score, MCC, kappa, and error rate to a few other existing techniques in order to validate its performance. Currently, accessible methods include Multi-Layer Perceptrons (MLP), Random Forest (RF), Decision Trees (DT), and Support Vector Matrix (SVM). A brief explanation of the proposed and existing models performance metrics comparison are as follows.

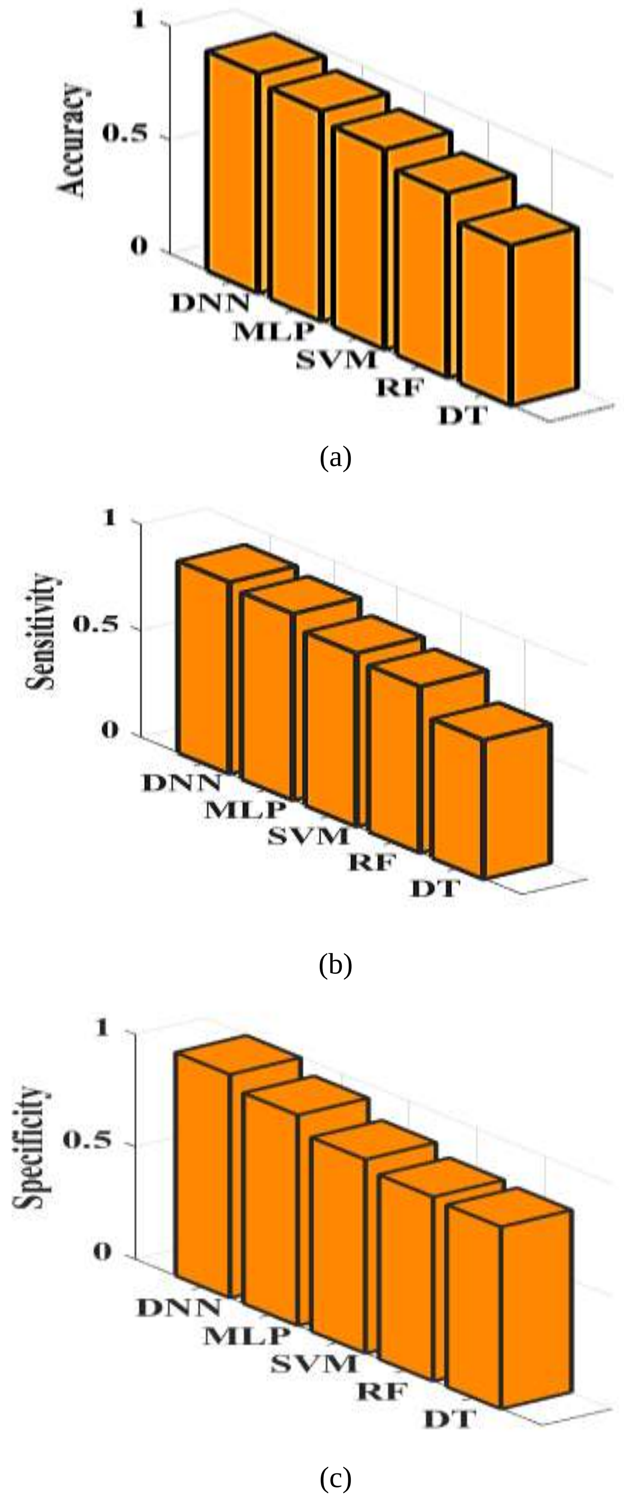

Figure 5. *Comparison of proposed and existing methods (a) accuracy (b) sensitivity(c) specificity.*

An accurate system is one that can predict a value with the least amount of error. Figure 5(a) illustrates the accuracy of the suggested and current methods. The suggested approach has an accuracy rate of 97%, while MLP, SVM, RF, and DT have rates of 90%, 60%, 50%, and 40%, respectively. The suggested model is more effective than the current approaches. Figure 5(b) compares the suggested and current techniques sensitivity. It is known what the ratio is between what is truly positive and precisely positive. The sensitivity of the suggested approach is 80%, MLP is 70%, SVM is 50%, RF is 40%, and DT is 30%. Figure 5(c) compares the specificity of recommended and current techniques. A model's specificity indicates how well it can predict actual negatives of all possible types. In comparison to various current approaches, such as MLP, SVM, RF and DT with corresponding specificity values of 80%, 60%, 50% and 48%, the proposed method's specificity value was determined to be 97%.

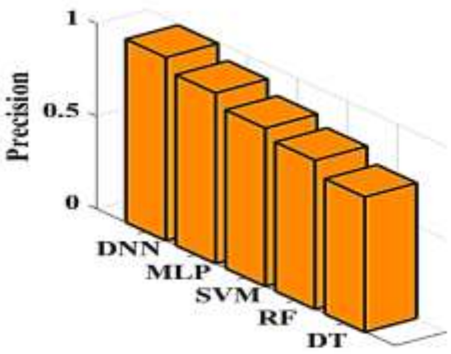

(a)

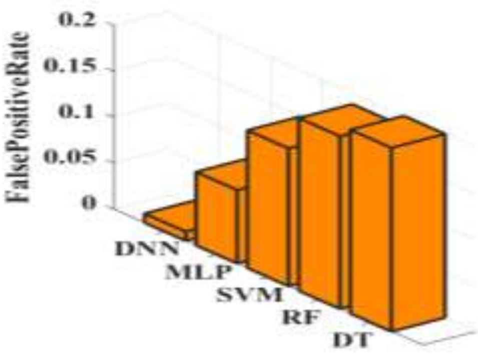

(b)

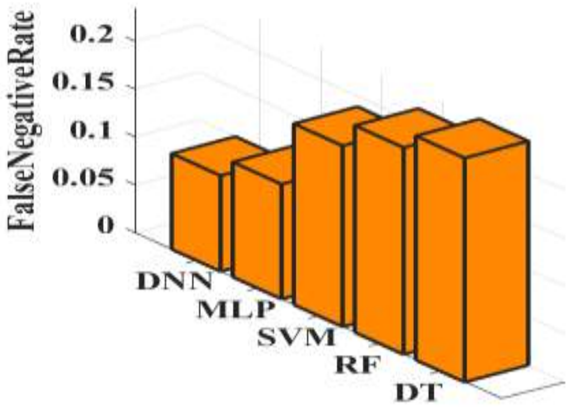

(c)

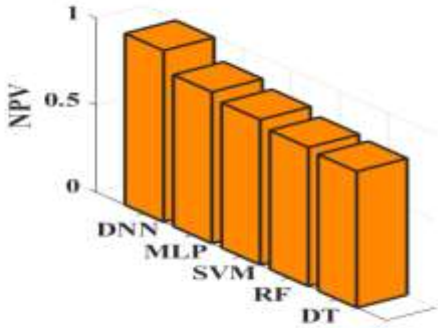

(d)

Figure 6. *Comparison of proposed and existing methods (a) precision (b) false positive rate(c) false negative rate (d) NPV.*

Figure 6(a) compares the precision of the suggested method with the current one. The number of positive events that may be reliably predicted is typically used in measurements to ensure accuracy. In comparison to other current approaches, such as MLP, SVM, RF and DT with corresponding precision values of 70%, 50%, 48%and 30%, the suggested method's precision value was discovered to be 90%. The false positive rate for the recommended and current approaches is contrasted in Figure 6(b). The false positive rate computes the quantitative probability of each positive test result or each negative test result that results in a positive test result because of a defect. The proposed method has a false positive rate of 0.002%, while the current MLP has a rate of 0.04%, SVM's is 0.1%, RF's is 0.12%, and DT's is 0.13%. The false negative rate contrast between the recommended and current approaches is shown in Figure 6(c). The proposed method have false negative rate is 0.07%, the existing MLP have 0.08%, SVM have 0.12%, RF have 0.13% and DT have 0.13%. In order to determine the prospect that people with a negative screening test are indeed illness, negative predictive value concentrates on subjects with a negative test result, as shown in Figure 6(d). The proposed method NPV is 90% existing method MLP is 70%, SVM is 58%, RF is 49% and DT is 47%.

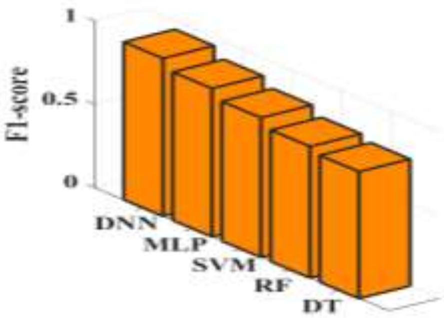

(a)

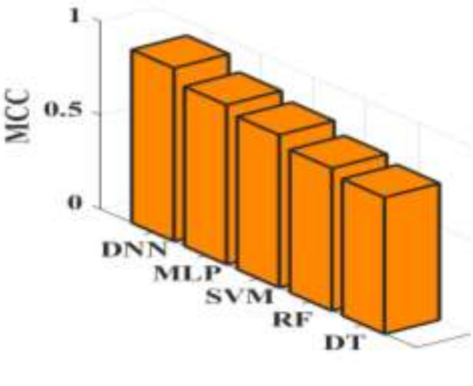

(b)

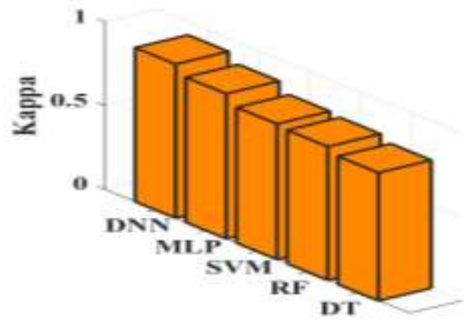

(c)

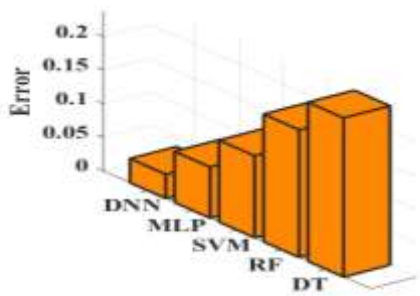

(d)

Figure 7. *Comparison of proposed and existing methods (a) F1 _score (b) MCC (c) kappa (d) error.*

The value of the F1 Score is then examined for both the suggested and existing methods. The F1_ score is statistically analyzed to reveal the binary types of the system and the accuracy level of the data collection. Figure 7 (a) displays a comparison of the suggested and current F1 Score. For the suggested technique, the F1 Score values are 88%, 80% for MLP, 52% for SVM, 48% for RF, and 46% for DT. To assess or measure the difference between expected and actual results, one uses Matthews' correlation coefficient (MCC). The values for MCC, MLP, SVM, RF, and DT in the recommended technique are 89%, 70%, 58%, and 46%, respectively, as shown in Figure 7(b). Figure 7(c) illustrates the kappa comparison between the proposed and current methods. A statistical indicator of the reliability of various variables at various rates is called kappa. Kappa is 88%, MLP is 70%, SVM is 49%, RF is 48%, and DT is 47% for the suggested approach. The error values of the proposed and existing approaches are then compared. The number of errors or problems a system has is measured by its error level. When the error is high, the system operates worse; when the error is low, the system operates more efficiently. Figure 7 (d) presents an error comparison of the proposed and current methodologies. The error rates for the suggested approach are 0.03%, 0.05 for MLPs, 0.06 for SVMs, 0.11% for RFs, and 0.15% for DTs.

1.7. Comparison of feature extraction performance

To validate the performance of accuracy, sensitivity, specificity, and error, the suggested feature extraction performance is compared to a few other current methods in this section. The two most common techniques for extracting features at the moment are Local Binary Pattern (LBP) and Histogram Oriented Gradient (HOG) [34]. The following was a brief discussion of the performance comparison.

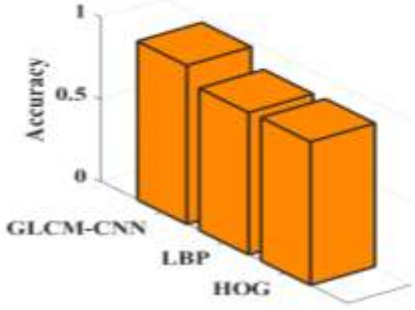

(a)

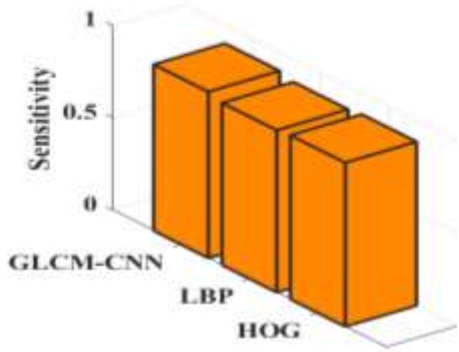

(b)

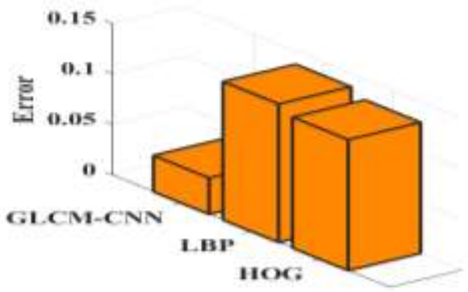

(c)

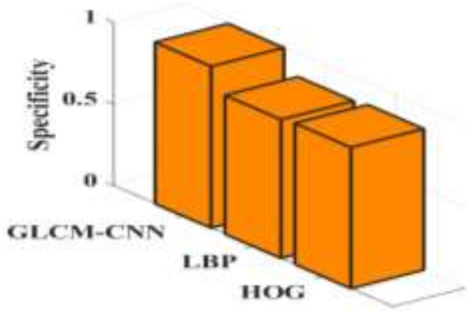

(d)

Figure 8. *Comparison of proposed and existing extraction methods (a) accuracy (b) sensitivity(c) error (d) specificity*.

The system that can foresee a value with the least degree of error is the one that determines the accuracy of extraction. In Figure 8(a), the accuracy of the suggested and current feature extraction techniques is shown. The accuracy rate of the suggested approach is 97%, while LBP is 75% and HOG is 60%. The suggested feature extraction method offers a more effective working process as compared to the current ones. Figure 8(b) compares the suggested and current feature extraction methodologies sensitivity. LBP is 65%, HOG is 60%, and the suggested feature extraction sensitivity is 85%. A feature error comparison between the suggested and current techniques is presented in Figure 8(c). The error rate of the suggested approach is 0.03%, LBP's is 0.09%, and HOG's is 0.07%. Figure 8(d) compares the specificity of proposed and current feature extraction techniques. In comparison to various current approaches, such as LBP and HOG with corresponding specificity values of 60% and 55%, the proposed method's specificity value was determined to be 97%. The comparative analysis of feature extraction demonstrates that the proposed fusion approach provides a better outcome than the existing approaches.

1.8. Computational timing analysis

The duration of time needed to complete a computing process is known as the computation time. Computational timing analysis includes training and testing timing. Training time defines the period of time during which an algorithm trains a model using training data. The testing period is to check a trained model to effectively work or not. A classifier uses a trained model to make predictions during the test period. The below section clearly explains about training and testing time.

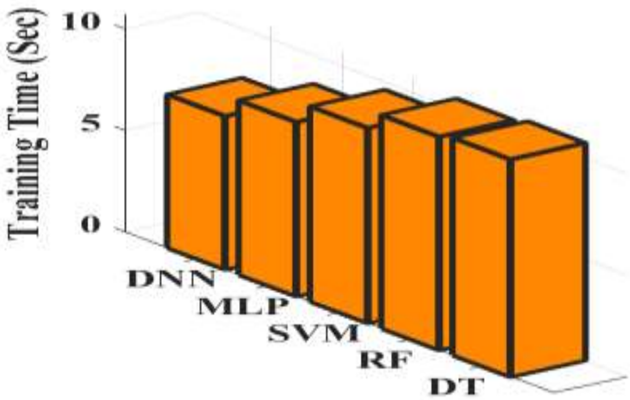

(a)

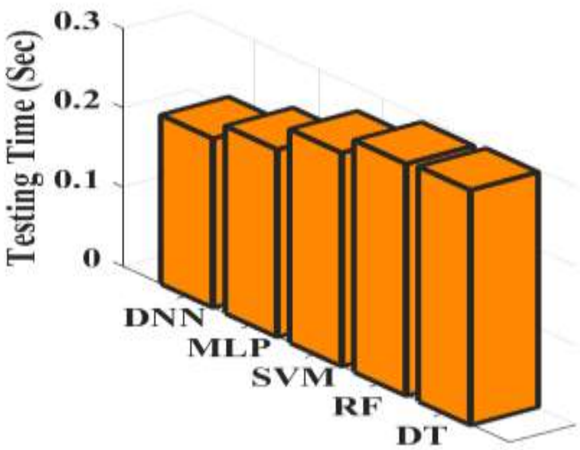

(b)

Figure 9. *computational timing analysis of (a) Training time and (b) testing time.*

Figure 9 compares the training and testing times of the suggested and current methods. The proposed method's training time is 6 sec, MLP's training time is 7 sec, SVM's training time is 7sec, RF's training time is 6.5sec and DT's training time is 6.5sec. The proposed method's testing time is 0.19 sec, MLP's testing time is 0.2 sec, SVM's testing time is 0.21%, RF's testing time is 0.22% and DT's testing time is 0.22%.

1.9. Comparative analysis

This section compares the performance of the suggested model with a few other recently created validation techniques. Accuracy, precision, specificity, NPV, and F1_score are only a few of the performance indicators used to evaluate a task as shown in Table 4. The comparison was held on various classifier osteoporosis prediction metrics, the existing classifiers are considered as google net, efficient net b3, efficient net b4, ResNet 34, and ResNet 18.

Table 4. *Comparative analysis of existing methods [35]*

Performance metrics	**Accuracy**	**Precision**	**Specificity**	**NPV**	**F1_score**
Google net	0.8584	0.8966	0.8824	0.8182	0.8667
Efficient net b3	0.8850	0.9016	0.8824	0.8654	0.8943
Efficient net b4	0.8584	0.8594	0.8235	0.8571	0.8730
ResNet 34	0.8673	0.9273	0.9216	0.8103	0.8718
ResNet 18	0.8407	0.8667	0.8431	0.8113	0.8525
Proposed	0.97	0.90	0.97	0.90	0.88

Table 4 shows that the suggested model outperforms the different network classifiers in terms of performance. While the existing Google Net, Efficient Net B3, Efficient Net B4, ResNet 34, and ResNet 18 have 0.85, 0.88, 0.85, 0.86, and 0.84 accuracy, the suggested DNN model has 0.97 accuracy. Same as precision, specificity, NPV and F1_score also compared, in that also the proposed model provides a better outcome.

Table 5. *Comparative analysis of existing methods [36]*

Performance metrics	**Accuracy**	**Sensitivity**
VGG16 network	95%	96%
Proposed	97%	97%

In Table 5, VGG16 network performance metrics include accuracy and sensitivity is noted and compared to the proposed model. The comparison shows the proposed model offers a better prediction outcome as well as provides a rapid process to diagnose osteoporosis. The novel features fusion strategy provides accurate features from the images and the text-image fusion offers a reliable prediction performance [37-39].

5. Conclusion

An advanced fusion strategy with a contrast enhancement approach was developed to detect the osteoporosis disease properly. Typically, DEXA approaches were utilized to diagnose osteoporosis which find the BMD value of a bone to make an easy diagnosis process. But it was not provide a reliable operation at all time as well as more cost. So, medical images were utilized to detect osteoporosis, yet that also have some limitations for detecting disease. The exact condition of the bone was identified by analyzing both BMD and X ray images. In the proposed model, a novel feature fusion and feature subject fusion model was developed to diagnosis the disease in the femur bone. In the proposed model, the femurs right and left bones images were utilized to examined the disease. For a detailed prediction, separate the subject record from the image data. Pre-processing was done on the image data since they contain noise and other unwanted components that could complicate prediction. The augmentation process was utilized to increase prediction accuracy. Convolutional feature extraction and GLSDM were used to extract the features from the augmented data individually. To combine extracted features with the subject record using a fusing technique. The fused data is analyzed using a DNN classifier, which predicts the proper status of the given dataset. The proposed approach provides a better prediction performance with low processing time. The proposed model provide 97% accuracy, 90% precision, 88% F1 _score, and 7% false positive rate. The suggested approach performs similarly to other modern methods like MLP, SVM, RF, and DT. In future, osteoporosis will be diagnosis in femur bone using ensemble methods to reduce computational expensive.

Acknowledgement

Funding: The authors declare that no funds, grants, or other support were received during the preparation of this manuscript.

Conflict of Interest: The authors declared that they have no conflicts of interest to this work. We declare that we do not have any commercial or associative interest that represents a conflict of interest in connection with the work submitted.

Availability of data and material: Not applicable

Code availability: Not applicable

Author contributions: The corresponding author claims the major contribution of the paper including formulation, analysis and editing. The co-author provides guidance to verify the analysis result and manuscript editing.

Compliance with ethical standards: This article is a completely original work of its authors; it has not been published before and will not be sent to other publications until the journal's editorial board decides not to accept it for publication.

References

[1] Rauner M, Taipaleenmäki H, Tsourdi E, Winter EM. Osteoporosis treatment with anti-sclerostin antibodies—mechanisms of action and clinical application. Journal of Clinical Medicine. 2021 Feb 16;10(4):787.

[2] Salech F, Marquez C, Lera L, Angel B, Saguez R, Albala C. Osteosarcopenia predicts falls, fractures, and mortality in Chilean community-dwelling older adults. Journal of the American Medical Directors Association. 2021 Apr 1;22(4):853-8.

[3] Hampson G, Stone M, Lindsay JR, Crowley RK, Ralston SH. Diagnosis and management of osteoporosis during COVID-19: systematic review and practical guidance. Calcified Tissue International. 2021 Oct;109(4):351-62.

[4] Beaudart C, Boonen A, Li N, Bours S, Goemaere S, Reginster JY, Roux C, McGowan B, Diez-Perez A, Rizzoli R, Cooper C. Patient preferences for lifestyle behaviours in osteoporotic fracture prevention: a

cross-European discrete choice experiment. Osteoporosis international. 2022 Jun;33(6):1335-46.

[5] LeBoff MS, Greenspan SL, Insogna KL, Lewiecki EM, Saag KG, Singer AJ, Siris ES. The clinician's guide to prevention and treatment of osteoporosis. Osteoporosis international. 2022 Oct;33(10):2049-102.

[6] Gonera-Furman A, Bolanowski M, Jędrzejuk D. Osteosarcopenia—The Role of Dual-Energy X-ray Absorptiometry (DXA) in Diagnostics. Journal of Clinical Medicine. 2022 Apr 30;11(9):2522.

[7] Yong EL, Logan S. Menopausal osteoporosis: screening, prevention and treatment. Singapore Medical Journal. 2021 Apr;62(4):159.

[8] Amphansap T, Rattanaphonglekha C, Vechasilp J, Stitkitti N, Apiromyanont K, Therdyothin A. Comparison of bone mineral density and vertebral fracture assessment in postmenopausal women with and without distal radius fractures. Osteoporosis and Sarcopenia. 2021 Dec 1;7(4):134-9.

[9] Fasihi L, Tartibian B, Eslami R, Fasihi H. Artificial intelligence used to diagnose osteoporosis from risk factors in clinical data and proposing sports protocols. Scientific Reports. 2022 Oct 31;12(1):18330.

[10] Ou Yang WY, Lai CC, Tsou MT, Hwang LC. Development of machine learning models for prediction of osteoporosis from clinical health examination data. International journal of environmental research and public health. 2021 Jul 18;18(14):7635.

[11] Burden AM, Tanaka Y, Xu L, Ha YC, McCloskey E, Cummings SR, Glüer CC. Osteoporosis case ascertainment strategies in European and Asian countries: a comparative review. Osteoporosis International. 2021 May;32(5):817-29.

[12] Xue Z, Huo J, Sun X, Sun X, Ai ST, LichiZhang, Liu C. Using radiomic features of lumbar spine CT images to differentiate osteoporosis from normal bone density. BMC Musculoskeletal Disorders. 2022 Apr 8;23(1):336.

[13] Erjiang E, Wang T, Yang L, Dempsey M, Brennan A, Yu M, Chan WP, Whelan B, Silke C, O'Sullivan M, Rooney B. Machine learning can improve clinical detection of low BMD: the DXA-HIP study. Journal of Clinical Densitometry. 2021 Oct 1;24(4):527-37.

[14] Jagadeesh A, Senthilkumar R. Bone Density Analysis and Osteoporosis Prediction Using Novel Convolutional Neural Network over Support Vector Machine Algorithm. Journal of Pharmaceutical Negative Results. 2022 Oct 7:1612-21.

[15] Ahern DP, McDonnell JM, Riffault M, Evans S, Wagner SC, Vaccaro AR, Hoey DA, Butler JS. A meta-analysis of the diagnostic accuracy of Hounsfield units on computed topography relative to dual-energy X-ray absorptiometry for the diagnosis of osteoporosis in the spine surgery population. The Spine Journal. 2021 Oct 1;21(10):1738-49.

[16] Liao PH, Tsuei YC, Chu W. Application of Machine Learning in Developing Decision-Making Support Models for Decompressed Vertebroplasty. InHealthcare 2022 Jan 23 (Vol. 10, No. 2, p. 214). MDPI.

[17] Wu Q, Nasoz F, Jung J, Bhattarai B, Han MV, Greenes RA, Saag KG. Machine learning approaches for the prediction of bone mineral density by using genomic and phenotypic data of 5130 older men. Scientific Reports. 2021 Feb 24;11(1):4482.

[18] Prakash UM, Kottursamy K, Cengiz K, Kose U, Hung BT. 4x-expert systems for early prediction of osteoporosis using multi-model algorithms. Measurement. 2021 Aug 1;180:109543.

[19] Jang R, Choi JH, Kim N, Chang JS, Yoon PW, Kim CH. Prediction of osteoporosis from simple hip radiography using deep learning algorithm. Scientific reports. 2021 Oct 7;11(1):19997.

[20] Sato Y, Yamamoto N, Inagaki N, Iesaki Y, Asamoto T, Suzuki T, Takahara S. Deep learning for bone mineral density and T-score prediction from chest X-rays: A multicenter study. Biomedicines. 2022 Sep 19;10(9):2323.

[21] Sollmann N, Löffler MT, Kronthaler S, Böhm C, Dieckmeyer M, Ruschke S, Kirschke JS, Carballido- Gamio J, Karampinos DC, Krug R, Baum T. MRI- based quantitative osteoporosis imaging at the spine and femur. Journal of Magnetic Resonance Imaging. 2021 Jul;54(1):12-35.

[22] Yamamoto N, Sukegawa S, Yamashita K, Manabe M, Nakano K, Takabatake K, Kawai H, Ozaki T, Kawasaki K, Nagatsuka H, Furuki Y. Effect of patient clinical variables in osteoporosis classification using hip x-rays in deep learning analysis. Medicina. 2021 Aug 20;57(8):846.

[23] Du J, Wang J, Gai X, Sui Y, Liu K, Yang D. Application of intelligent X-ray image analysis in risk assessment of osteoporotic fracture of femoral neck in the elderly. Mathematical Biosciences and Engineering. 2023 Jan 1;20(1):879-93.

[24] Dadsetan S, Kitamura G, Arefan D, Guo Y, Clancy K, Yang L, Wu S. Machine Learning and Radiomics for Osteoporosis Risk Prediction Using X-ray Imaging. medRxiv. 2022 Feb 3:2022-02.

[25] Shahzad M, Khan TF, Bashir M, Ayub M, Ashraf F, Hashmi S, Zahoor F, Jaskani FH. DETECTION OF OSTEOPOROSIS IN DEFECTED BONES USING RADTORCH AND DEEP LEARNING TECHNIQUES. International Journal of Engineering Applied Sciences and Technology. 2021;6(4):2455-143.

[26] Slaidina A, Nikitina E, Abeltins A, Soboleva U, Lejnieks A. Gray values of the cervical vertebrae detected by cone beam computed tomography for the identification of osteoporosis and osteopenia in postmenopausal women. Oral Surgery, Oral Medicine, Oral Pathology and Oral Radiology. 2022 Jan 1;133(1):100-9.

[27] Hsu PC, Luzhbin D, Shih TY, Wu J. Diagnosis of Osteoporosis by Quantifying Volumetric Bone Mineral Density of Lumbar Vertebrae Using Abdominal CT Images and Two-Compartment Model. InHealthcare 2023 Feb 13 (Vol. 11, No. 4, p. 556). MDPI.

[28] Aksoy B, Salman OK. A New Hybrid Filter Approach for Image Processing. Sakarya University Journal of Computer and Information Sciences. 2020 Dec 30;3(3):334-42.
[29] Routray S, Malla PP, Sharma SK, Panda SK, Palai G. A new image denoising framework using bilateral filtering based non-subsampled shearlet transform. Optik. 2020 Aug 1;216:164903.
[30] Alkhalid FF, Hasan AM, Alhamady AA. Improving radiographic image contrast using multi layers of histogram equalization technique. IAES International Journal of Artificial Intelligence. 2021 Mar 1;10(1):151.
[31] Yang A, Yang X, Wu W, Liu H, Zhuansun Y. Research on feature extraction of tumor image based on convolutional neural network. IEEE access. 2019 Feb 3;7:24204-13.
[32] Benco M, Kamencay P, Radilova M, Hudec R, Sinko M. The comparison of color texture features extraction based on 1D GLCM with deep learning methods. In2020 International Conference on Systems, Signals and Image Processing (IWSSIP) 2020 Jul 1 (pp. 285-289). IEEE.
[33] Shabri A, Samsudin R, Yusoff Y. Combining deep neural network and fourier series for tourist arrivals forecasting. InIOP Conference Series: Materials Science and Engineering 2020 May 1 (Vol. 864, No. 1, p. 012094). IOP Publishing.
[34] Yamamoto N, Sukegawa S, Kitamura A, Goto R, Noda T, Nakano K, Takabatake K, Kawai H, Nagatsuka H, Kawasaki K, Furuki Y. Deep learning for osteoporosis classification using hip radiographs and patient clinical covariates. Biomolecules. 2020 Nov 10;10(11):1534.
[35] Dzierżak R, Omiotek Z. Application of deep convolutional neural networks in the diagnosis of osteoporosis. Sensors. 2022 Oct 26;22(21):8189.
[36] Al-Shara NA, Al-khulaidi NA. Long Bone Fracture Detection Using Machine Learning. Progress in Engineering Application and Technology. 2022 Dec 19;3(2):998-1008.
[37] Manohar Madgi, Shantala Giraddi, Geeta Bharamagoudar, MS Madhur, Brain tumor classification and segmentation using deep learning, 2021, Smart Computing Techniques and Applications: Proceedings of the Fourth International Conference on Smart Computing and Informatics, Springer Singapore, Volume 2, Pages 201-208.
[38] Murigendrayya M. Hiremath B.V. Suma, S.M. Chandra Shekar, Praveena Mydolalu Veerappa, Swapnil S. Ninawe, Krishnan Bandyopadhyay, Improving Network Lifetime for Cluster Based WSN through Energy Aware Routing, 2023, International Journal of Electronics and Communication Engineering, Volume 10, Issue-11, Pages-6.
[39] Murigendrayya M Hiremath Vishwanatha K, Advanced Motion Detection Algorithm for Patient Monitoring using Cell Phone with Video Display, 2012, International Journal of Electronics Signals and Systems, Volume-1, Issue-4.